

Characterization of Cationic Diarylethene by Electron Spin Resonance and Absorption Spectra—Ratio of Open/Closed-Ring Isomers

Satoshi Yokojima,^{*,†} Kenji Matsuda,[‡] Masahiro Irie,[‡] Akinori Murakami,[†]
Takao Kobayashi,[†] and Shinichiro Nakamura^{*,†}

Mitsubishi Chemical Group, Science and Technology Research Center, Inc. and CREST-JST, 1000
Kamoshida-cho, Aoba-ku, Yokohama, 227-8502 Japan, and Department of Chemistry and Biochemistry,
Graduate School of Engineering, Kyushu University, Hakozaki 6-10-1, Higashi-ku, Fukuoka 812-8581, Japan

Received: January 31, 2006

Electrochemical cyclization/cycloreversion reactions of a diarylethene, 1,2-bis(3-methyl-2-thienyl)perfluorocyclopentene, are examined experimentally by electron spin resonance (ESR) and absorption spectra. To understand the ESR spectrum, the hyperfine coupling constants are calculated by the density functional theory (DFT) with the B3LYP exchange-correlation functional. The averaged values of the hyperfine coupling constants are approximated by imposing the C_2 symmetry on the structure of the diarylethene. We found that the spectral width of the ESR is significantly different between the open- and closed-ring isomers. This is due to the difference in the π -conjugation between two isomers. The ESR spectral width analysis could, thus, be used to identify the isomerization of the radical species, which involve the change of the π -conjugation. The experimentally observed spectrum is found to be the mixture of the open- and closed-ring isomers of the diarylethene. The excitation energies of the cationic diarylethenes are further identified by the SAC-CI calculations.

1. Introduction

In chemistry, biology, and material science, magnetic resonance spectroscopy is extensively studied.¹ For the determination of molecular structures and the monitor of chemical reactions, the magnetic resonance spectroscopy is used as one of the standard methods. NMR spectroscopy of small molecules, biological systems such as proteins, polymers, and clusters are considered to be one of the indispensable data owing to its abundant information from the charts of chemical shifts, coupling constants, and relaxation times.² Theoretical chemistry has provided useful aids for the practical applications of NMR data. Examples include the GIAO, IGLO, and the Karplus's equation of J coupling.³ On the other hand, ESR spectroscopy, although in itself, contains also rich information of the molecular properties, the application in chemistry and biology is rather limited. One of the reasons for the limitation is reduced to be the difficulty of the interpretation (convolution) of the hyperfine coupling constants (hfcc's) and g values. For the realization of this rich potentiality of ESR data, again theoretical contribution is in order.

This paper reports on a theoretical study in this regards. We have chosen a problem of the product assignment of the electrochemical reactions of a diarylethene. Diarylethene molecules are one of the candidates of molecular devices, such as the molecular switches and memories.⁴ Diarylethene derivatives have two thermally stable structures, i.e., open- and closed-ring isomers. (See Figure 1.) The open-ring isomer is converted to the closed-ring isomer upon irradiation with UV light. Similarly, the open-ring isomer is obtained from the closed-

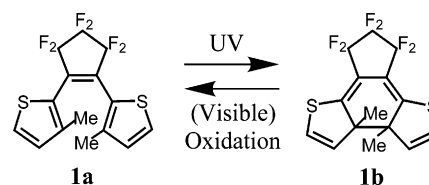


Figure 1. The open-ring isomer diarylethene derivative, 1,2-bis(3-methyl-2-thienyl)perfluorocyclopentene (**1a**) and the corresponding closed-ring isomer (**1b**).

ring isomer upon irradiation with visible light.⁴ Due to the distinctive difference in structure, especially the difference in the π -conjugation, they have different absorption spectra. Since we can control the structure optically, it is adequate to use it as the molecular switches or memories.⁴

The control of the structure, however, can be performed not only by the optical method but also by the oxidation/reduction.⁵ Unlike the optical cyclization/cycloreversion reactions of diarylethenes, the electrochemical cyclization/cycloreversion reactions of diarylethenes have not been studied well.

Previously, we have reported that during the electrolysis of the closed-ring isomer, a new band ($\lambda_{\max} = 667$ nm) appeared and diminished after the electrolysis was stopped, which was assigned as the cation radical of the closed-ring isomer.⁶

In this paper, we further characterize the structure of the cationic diarylethene by ESR and absorption spectra. The hfcc's are calculated by the density functional theory with the B3LYP⁷ exchange-correlation functional. The B3LYP is successfully applied to calculate the hfcc for many systems.^{8–10} The careful examination of the ESR spectrum shows that the signal is the mixture of the open- and closed-ring isomers of the diarylethene. The peak energy of the cationic diarylethene was identified by the SAC-CI calculations. The ratio of the open/closed-ring isomers in the reaction process is thus determined.

* Corresponding authors phone: +81-45-963-3833 and fax: +81-45-963-3835 (S.Y.) and (S.N.); e-mail: yokojima@rc.m-kagaku.co.jp (S.Y.) and shin@rc.m-kagaku.co.jp (S.N.).

[†] Mitsubishi Chemical Group and CREST-JST.

[‡] Kyushu University.

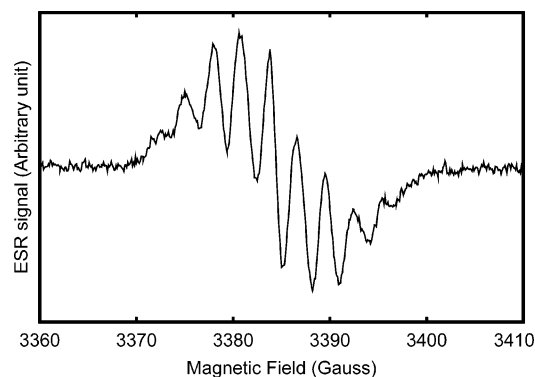


Figure 2. ESR spectrum of **1b** under electrolysis (+1.1 V vs Au reference electrode) measured in dichloromethane (1×10^{-3} M) at room temperature. $g = 2.0072$.

2. Experiments

The molecule studied was 1,2-bis(3-methyl-2-thienyl)perfluorocyclopentene (**1a**) (Figure 1).⁶ After irradiation with UV light, the photogenerated closed-ring isomer **1b** (Figure 1) was separated using HPLC in the dark. The X-band ESR spectrum under electrolysis of the isolated pure closed-ring isomer was measured in dichloromethane solution (Figure 2). The working and reference electrodes were Au, and the counter electrode was Pt. The supporting electrolyte was tetrabutylammonium perchlorate. The electrolysis was performed at 1.1 V (vs Au reference electrode). At this potential, only the closed-ring isomer was oxidized. The observed spectrum was the 9-line hyperfine-coupled signal centered at $g = 2.0072$. This suggests that the intermediate of the oxidative ring-opening reaction is a monocation radical.

This intermediate was also observed by absorption spectroscopy along with the electrolysis of the closed-ring isomer (Figure 3). Upon electrolysis of the solution of the closed-ring isomer in acetonitrile at 1.4 V (vs Ag/Ag⁺) the new absorption band ($\lambda_{\max} = 667$ nm) appeared (Figure 3(a)), and it diminished after the electrolysis was stopped (Figure 3(b)). Figure 3 also indicates that there is another new absorption band above 800 nm.

3. Computational Method

Because the ESR experiment is performed in the dichloromethane solvent, the isotropic hfcc has to be calculated. The calculation of the isotropic hfcc requires high accuracy. Many methods are tested, and the DFT with the B3LYP⁷ exchange-correlation functional or the calculations with the CCSD¹¹ types are found to be reliable if the triple- ζ or higher basis sets are used.⁸ The hfcc's of the fluorine atoms in the aromatic molecules are studied by the B3LYP and found to be a good correlation with experiments.

We have, thus, calculated the hfcc's by the unrestricted B3LYP hybrid density functional method^{7,12,13} in Gaussian 03.¹⁴ We have used the cc-pVDZ, cc-pVTZ,¹⁵ and 6-311+G(2df,p)¹⁶ basis sets. The geometries are optimized by the unrestricted B3LYP calculation with the cc-pVTZ basis set.

In addition to the requirement for these high level calculations, the structural deformation of diarylethenes complicates the identification of the ESR spectra. The five-membered carbon ring causes the puckering. Moreover, the two methyl groups might rotate at room temperature, i.e., many potential energy minima can exist. The vibrational effect on the hfcc's is intensively studied for small molecules, such as methyl and fluoromethyl radicals.¹⁷ In these studies, the values of the hfcc's are averaged over the path of vibration, and the ensemble

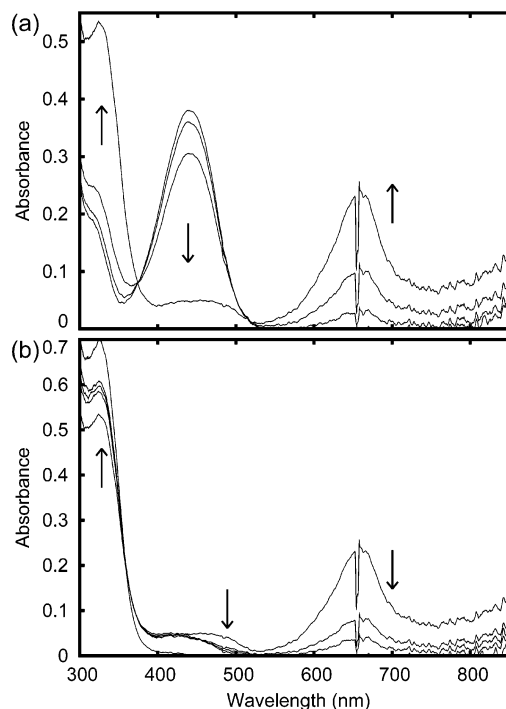


Figure 3. (a) Change of the absorption spectrum of the closed-ring isomer by electrolysis at 1.4 V (Ag/Ag⁺) (acetonitrile, 1×10^{-3} M). Closed-ring isomer **1b**, after electrolysis for 30 s, 60 s, and 120 s. (b) Change of the absorption spectrum of the closed-ring isomer after the measurement of (a). Initial, 20 s, 40 s, 120 s, and the open-ring isomer **1a**.

average is calculated over the vibrational modes. However, this has been done for small molecules or molecules with high symmetries. The existence of many potential energy minima requires the analysis of the full potential energy surface as well as the analysis of the rate from one potential minimum to the others in order to determine whether the rate is faster than the ESR time scale. These calculations are very expensive. Instead, we rather simply averaged hfcc's by employing a C_2 symmetric structure. The justification of this simplification will be explained in the discussion.

The ESR spectrum is calculated by using the derivative of the Gaussian profile

$$S(H) = -2C \sum_k \frac{H - \xi_k}{\eta} \exp\left(-\left(\frac{H - \xi_k}{\eta}\right)^2\right) \quad (1)$$

where C is a constant, η is a parameter for the spectral line width, and ξ_k is given by the isotropic hfcc a_i of the i th atom with a nuclear spin of 1/2 (F or H).

$$\xi_k = \sum_{i=1}^N (-1)^{\alpha_i^k} \frac{a_i}{2} \quad (2)$$

Here, α_i^k is 0 or 1, N is the total number of atoms with a nuclear spin of 1/2, and k runs from 1 to 2^i . A different set of values for α_i^k ($i = 1, \dots, N$) is assigned for each k . In the following calculations, $\eta = 0.45$ G is used.

The SAC-CI method¹⁸ implemented in Gaussian 03 is used for the calculation of the absorption spectra. The accuracy level of the SAC-CI calculation has been set to LevelOne. The 6-31G-(d) basis set is used for the S atom and the 6-31G for other atoms. The structures of the diarylethene are optimized by the B3LYP/cc-pVDZ with keeping the C_2 symmetry. To confirm

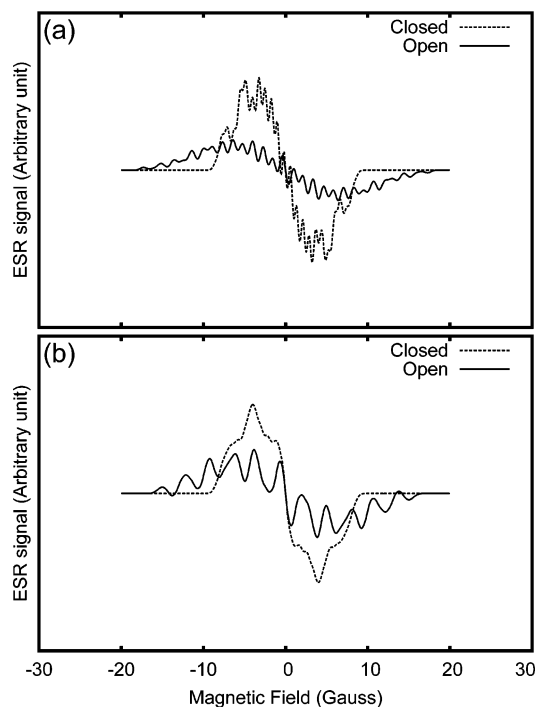


Figure 4. ESR spectra (computational results). (a) The most stable structure of diarylethene, i.e., no symmetry is imposed. (b) The structure of diarylethene with the C_2 symmetry. The cc-pVTZ basis set is used. Dashed line: ESR spectrum of the closed-ring isomer. Solid line: ESR spectrum of the open-ring isomer.

the calculation, we further perform the TDDFT calculation¹⁹ with the B3LYP hybrid density functional with the 6-31G(d) basis set. In this case, we use the two structures, i.e., the C_2 symmetric structure and the most stable structure without imposing symmetry. Both structures are optimized by the B3LYP/cc-pVDZ.

4. Results and Discussion

4.1. Identification of Structure by ESR Spectra. The calculated ESR spectra of the most stable structures of the diarylethene open/closed-ring isomers are shown in Figure 4(a). Because 10 H atoms and 6 F atoms have nonzero hfcc's, the ESR spectra become complicated. The spectra have many more peaks than the experimentally observed ESR spectrum, Figure 2. On the other hand, the ESR spectra with the C_2 symmetric structures are much simpler. (See Figure 4(b).) We have obtained a fewer number of peaks in Figure 4(b), but we still see the discrepancies between the observed and calculated ESR spectra.

The difference in the ESR spectra due to the difference of the structure is mainly due to the fact that many hfcc's with

different values are contributing to the ESR spectra. The most stable structure slightly deviates from the C_2 symmetric structure.²⁰ Therefore, all the hfcc's at 16 atoms have different values, which results in a lot of peaks in the calculated ESR spectra. However, these peaks are artificial. The structure of this molecule fluctuates not only around the structure of the lowest energy but also around other minima. The electronic energy difference of the optimized structure with and without the C_2 symmetry is only 1.14 (0.89) kcal/mol for the closed-ring (open-ring) isomer. The large difference of the hfcc's between the structures with and without the C_2 symmetry is mainly found in the fluorine atom whose position is strongly affected by the puckering. Therefore, the averaging of the hfcc over the puckering is required. As is well-known, the ESR spectrum also depends on the rotation of the methyl groups and the basis set. Even though these are known issues, to understand the following analysis more clearly for this system, we show the dependence of the hfcc's on the rotation of the methyl groups and the basis set dependence of the ESR spectra in the Supporting Information.

Although the ESR spectra depend on the choice of the basis set, the hfcc's are approximately similar as shown in Table 1, i.e., the small value of the hfcc's for a basis set is kept to be small for other basis sets. This is reflected on the ESR spectral width W .²¹

$$W = \sum_i |a_i| \quad (3)$$

Since we are interested in the difference of the ESR spectra between the open- and closed-ring isomers, the spectral width W , rather than each a_i , is more useful to characterize them. The calculated spectral width of the closed-ring isomer is about 17–19 G, which is much smaller than the observed spectral width of 32 G. On the other hand, the spectral width of the open-ring isomer is about 28–32 G, which is consistent with the experimental value. The spectral width W of minimum energy structures also gives similar values for a large basis set, i.e., 17.13 and 35.03 G for the closed- and open-ring isomers for the cc-pVTZ basis set, respectively. However, the ESR spectrum of the open-ring isomer fails to reproduce the distribution of the peak intensity. The computational results show the similar peak intensity extends over the spectrum, whereas the experimental peaks are larger around the center of the spectrum.

The experimental spectra can only be explained as the mixture of the open- and closed-ring isomers. Because the spectral width of the closed-ring isomer is smaller than that of the open-ring isomer, the peak intensity around the center of the ESR spectrum is enhanced by the mixture, which is consistent with the experimental spectrum.

The reaction scheme is given by the following processes: (i) oxidation of the closed-ring isomer by the electrolysis, (ii)

TABLE 1: Hyperfine Coupling Constant (Gauss)^a

basis set	H1	H2	H3	H4	H5	F1	F2	F3	W^b	
				closed						
6311+G(2df,p)	-0.04	-1.99	0.59	0.13	-0.66	1.52	4.13	-0.25	18.64	
cc-pVDZ	0.04	-1.99	0.47	0.12	-0.62	1.22	4.69	-0.33	18.94	
cc-pVTZ	0.19	-2.13	0.58	0.11	-0.68	1.13	3.60	-0.26	17.39	
				open						
6311+G(2df,p)	-4.02	-0.74	1.90	2.59	-0.02	-0.71	3.62	0.76	28.71	
cc-pVDZ	-4.91	-0.11	1.94	3.19	0.21	0.62	3.47	1.11	31.11	
cc-pVTZ	-5.02	0.07	2.24	3.74	0.30	-0.53	3.20	0.67	31.56	

^a The structure is optimized by the unrestricted B3LYP/cc-pVTZ with the C_2 symmetry imposed. Because of the symmetry, the same value of the hfcc's appears twice. Thus, only half of them are shown in this table. The numbering of the atoms is shown in Figure 5. ^b The ESR spectral width W is defined in eq 3.

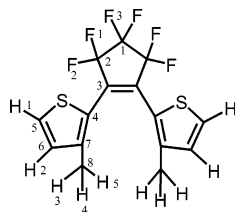


Figure 5. The numbering of the atoms.

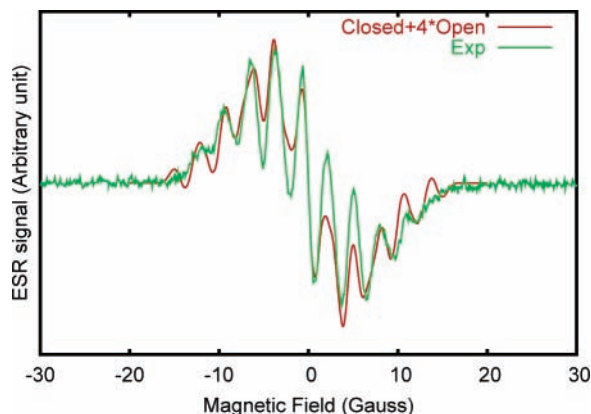


Figure 6. Same as Figure 4(b) but for the mixture of the open- and closed-ring isomers with a ratio of (open-ring isomer):(closed-ring isomer) = 4:1.

isomerization from the closed-ring to the open-ring isomers, and (iii) reduction of the radical cation open-ring isomer. The ratio between these two isomers will depend on the kinetics of the reaction. The computationally determined ratio of (open-ring isomer) vs (closed-ring isomer) is 4:1 as shown in Figure 6.

The spectral width is wider for the open-ring isomer than for the closed-ring one due to the difference in the π -conjugation between two isomers. The difference in the π -conjugation results in two effects on the hfcc's.

1. C7 of the open-ring isomer has a π -orbital unlike the closed-ring isomer. Therefore, the Mulliken atomic spin density on C7 of the open-ring isomer becomes larger (0.092) than that of the closed-ring isomer (-0.005). (See Figure 7.) Consequently, the hfcc's on H of the neighboring methyl group (H3–H5) of the open-ring isomer is larger than those of the closed-ring isomer as shown in Table 1.

2. The spin density on S has a large value (0.213) for the closed-ring isomer. This spin density moves to the neighboring C5 (0.211), and the spin density of S becomes small (-0.023) for the open-ring isomer. (See Figure 7.) Therefore, the hfcc for H1 for the open-ring isomer has a large value as shown in Table 1.

Both effects contribute to the wider spectral width for the open-ring isomer than for the closed-ring isomer. The first effect is expected from the change of the π -conjugation. But the second effect is not trivial. By considering the valence bond (VB) resonance structures, we can qualitatively understand why the spin density on S (or on C5) of the closed-ring isomer differs from that of the open-ring isomer. (See section 4.2 for the explanation.)

The detailed analysis of each hfcc and its relation to the ESR spectrum further supports that the radical cation observed in the ESR experiment is the mixture of the open- and closed-ring isomers. The number of the peaks of the ESR spectra is mainly characterized by the number of the large value of the hfcc's. The experimental coupling constants are about 2–3 G. Therefore, the hfcc's with more than 2 G should play an

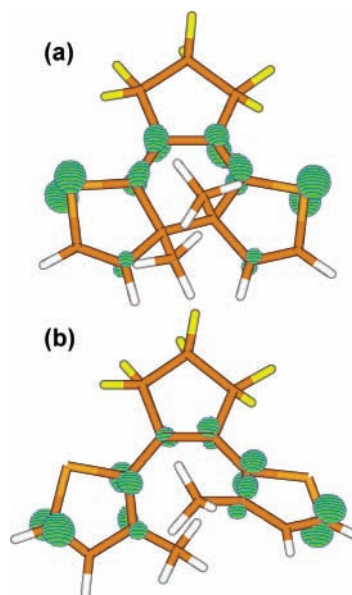


Figure 7. Spin density distribution for the diarylethene in the cationic state. (a) The closed-ring isomer. (b) The open-ring isomer. The spin contour is $0.01 e/(a_0)^3$ where a_0 is the Bohr radius.

important role in the spectrum. The closed-ring isomer has 4 hfcc's with more than 2 G. Note that only 2 such hfcc's (H2 and F2) are shown in Table 1 due to the C_2 symmetry. Because the hfcc of F2 is about twice of that of H2, the total number of the ESR peaks is 7, which is about the similar number of the experimentally observed ESR peaks, i.e., 7–9. However, the experimental coupling constant is about 2.9 G, which is much larger than the computational value of around 2 G for the closed-ring isomer. On the other hand, the open-ring isomer has 6–8 hfcc's with more than 2 G. Especially, 4 of them are more than 3 G. Therefore, the coupling constant or peak splitting is larger for the open-ring isomer than the closed-ring isomer. However, the existence of 6–8 large hfcc's result in the many peaks in the ESR spectra. As we found in Figure 4(b), there are 11 peaks for the open-ring isomer. By considering the mixture, the width of the spectrum is kept to be the open-ring isomer's one, but the peaks at the end of the spectrum are less pronounced and may be buried in the noise.

The hfcc's with large values are explained mostly by the spin density of the diarylethene. For example, the hfcc's of H2 of the closed-ring isomer with C_2 symmetric structure obtained by the B3LYP/cc-pVTZ can be explained as follows. The spin density on C6 is 0.0903, whereas the hfcc of H2 is -2.13 . Since most of the spin density is due to the π -electron, the value of hfcc agrees with the McConnell's relation.²² Please note that the difference of the spin density between the C_2 symmetric and the most stable structures is small compared to the difference of the spin density between the open- and closed-ring isomers.

4.2. VB Resonance Structures and Spin Density of Diarylethene. We can understand why the spin density is large on S for the closed-ring isomer and on C5 for the open-ring isomer by the resonance or delocalization energy. To explain it, the resonance structures of the closed- and open-ring isomers are shown in Figures 8 and 9, respectively.

As shown in Figure 8(b), the radical on S of the closed-ring isomer is stabilized by the delocalization of the positive charge. On the other hand, the radical on C5 of the closed-ring isomer is not favorable due to the existence of fewer resonance structures as shown in Figure 8(e). Although the resonance structures shown in Figure 8(f) are expected to have similar

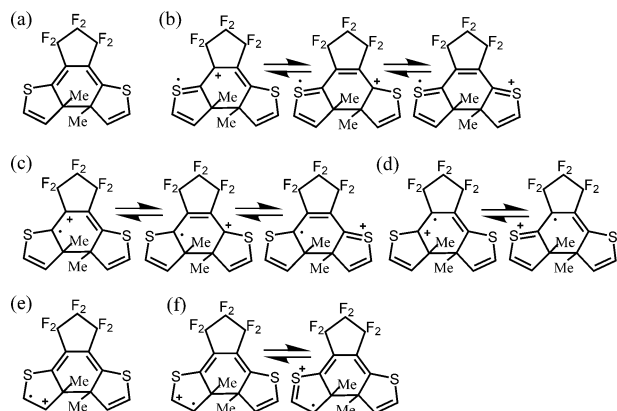


Figure 8. The resonance structures of the closed-ring isomer. (a) The neutral state. (b)–(f) The cationic state. The radical is on (b) S, (c) C4, (d) C3, (e) C5, and (f) C6.

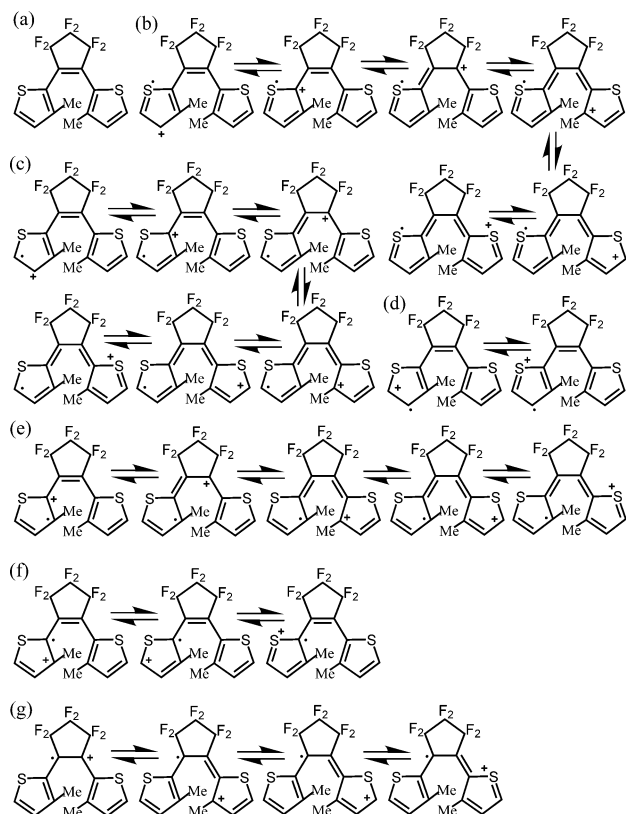


Figure 9. The resonance structures of the open-ring isomer. (a) The neutral state. (b)–(g) The cationic state. The radical is on (b) S, (c) C5, (d) C6, (e) C7, (f) C4, and (g) C3.

energy with that in Figure 8(e), the spin density on C6 is higher than that on C5 by the resonance between these structures.

The number of resonance structures increases significantly for the open-ring isomer, especially when the radical is on one of the double bonds. There are 6 resonance structures when the radical is on C5 as in Figure 9(c). The same number of resonance structures exists when the radical is on S of the open-ring isomer as in Figure 9(b). Here, the resonance structures shown in Figure 9(c) have similar energy with those in Figure 9(d)–(g) except for those in Figure 9(b). Therefore, the resonance structures in Figure 9(b) are less stabilized than those in Figure 9(c). This is why the spin density on C5 is larger but that on S is small for the open-ring isomer. It also explains the small hfcc of H2 of the open-ring isomer. This is due to the

small spin density on C6 which is caused by the fewer resonance structures in Figure 9(d).

The qualitative understanding provided by the VB resonance structure is further supported by examining the bond lengths. The bond lengths of S–C4 and S–C5 for the closed-ring isomer calculated by the B3LYP/cc-pVTZ are 1.755 and 1.776 Å, respectively. The corresponding cation radical has a shorter bond length for S–C4 (1.709 Å) but a similar bond length for S–C5 (1.769 Å). The shorter bond length of S–C4 for the cation radical of the closed-ring isomer is consistent with Figure 8(b) where S–C4 is a double bond. The bond lengths of S–C4 and S–C5 for the open-ring isomer are 1.751 and 1.715 Å, respectively. The corresponding cation radical has bond lengths similar to the neutral ones, i.e., S–C4 (1.767 Å) and S–C5 (1.700 Å). This is consistent with Figure 9(c).

4.3. Excitation Energies and Absorption Spectrum. First, to assess the computational accuracy, the absorption energy and oscillator strength are calculated for the neutral state by the SAC-CI. (See Table 2.) These computational results agree with the experimentally obtained excitation energies.²³ These results are also reproduced by the TDDFT. The validity of the use of the C_2 symmetric structure for the calculations of the excited states is assessed by the comparison between the excited states of the C_2 symmetric structure and those of the most stable structure using the TDDFT. The results obtained by the TDDFT indicate that the wavelengths and the oscillator strengths of the excited states change little by imposing the symmetry. Therefore, we assert that the characteristics of the excited states would not change by imposing the C_2 symmetry.

Next, we show that the excited-state energies obtained by the experimental absorption spectrum for the cationic diarylethene are reproduced by the SAC-CI. The calculated energy levels of the excited states and the corresponding oscillator strengths are shown in Table 3. The results obtained by the SAC-CI accurately reproduce the experimental absorption peak positions. From these results, we can assign the peak at the 667 nm is mainly due to the radical cation of the closed-ring isomer. The tail of the 667 nm peak for the longer wavelength may be due to the absorption of the radical cation of the open-ring isomer.

The results obtained by the TDDFT are less accurate in reproducing the excitation energies and sometimes give erroneous oscillator strengths. The failure to reproduce the oscillator strength by the TDDFT has been reported.^{24,25} As for the symmetry, imposing the C_2 symmetry on the cationic diarylethene only slightly affects the excitation energies in the TDDFT calculations. Therefore, like the diarylethene in the neutral state, we assert that the imposed symmetry in the SAC-CI calculation in Table 3 will not affect the results.

4.4. Parallel vs Antiparallel Structures for Open-Ring Isomer. The open-ring isomer has mainly two stable structures in thermal equilibrium, i.e., the parallel and antiparallel structures.^{26–28} In this study, we only show the ESR spectra of the antiparallel structure for the open-ring isomer due to the following reason. In general, the parallel structure of the open-ring isomer plays an important role on the photochromic reaction of diarylethene and has been investigated in relation to the quantum yield.^{26–28} Our previous study on the potential surface of this molecule²⁰ suggests that the two structures have similar energies. Therefore, we should find the contribution of the parallel structure of the open-ring isomer to the ESR spectrum if the system is in equilibrium. However, the calculated ESR spectrum for the most stable structure of the parallel open-ring isomer does not agree with the experimental one; the spectral

TABLE 2: Absorption Wavelength λ (Neutral Case)^a

symm	SAC-CI C_2			TDDFT C_2			TDDFT C_1		exp ^b
	λ (nm)	oscillator strength	symm	λ (nm)	oscillator strength	symm	λ (nm)	oscillator strength	
closed	462	0.1061	B	446	0.0803	B	446	0.0802	432
				324	0.0322	A	324	0.0323	
open	313	0.3401	B	338	0.2832	B	337	0.2852	316

^a The excitation energies less than 4 eV (310 nm) are shown. The symmetries of the ground states of the C_2 symmetric structure of the open- and closed-ring isomers are A. ^b Reference 23.

TABLE 3: Absorption Wavelength λ (Cationic Case)^a

symm	SAC-CI C_2			TDDFT C_2			TDDFT C_1		exp
	λ (nm)	oscillator strength	symm	λ (nm)	oscillator strength	symm	λ (nm)	oscillator strength	
closed	662	0.2030	B	762	0.0301	B	763	0.0379	667
	389	0.0497	A	597	0.1198	B	588	0.1123	
				479	0.0216	A	481	0.0231	
				404	0.0009	B	409	0.0016	
				399	0.0029	A	397	0.0023	
open	855	0.0581	A	932	0.0094	B	900	0.0079	850 ^{>}
	752	0.1661	A	817	0.0000	A	780	0.0011	
	719	0.0000	B	797	0.0751	B	761	0.0636	
	357	0.0471	B	460	0.0153	A	460	0.2699	
				448	0.2482	B	458	0.0287	
				420	0.0098	A	418	0.0101	
				374	0.0056	A	375	0.0066	
				356	0.0000	A	356	0.0011	

^a The excitation energies less than 3.5 eV (354 nm) are shown. The symmetries of the ground states of the C_2 symmetric structure of the open- and closed-ring isomers are B and A, respectively.

width is 40.97 G and the peak splitting is about 5 G. Thus, the existence of the parallel structure of the open-ring isomer rather gives a larger mismatch between the experimental and theoretical ESR spectrum.

There are two possible explanations for the apparent deviation of the calculated ESR spectrum for the parallel open-ring isomer from the experimental one.

(i) After the average of the hfcc over the puckering, the calculated ESR spectrum for the parallel structure becomes similar to the one for the antiparallel structure with the C_2 symmetry.

(ii) The isomerization of the cation radical open-ring isomer is much slower than the decay time of the cation radical to the neutral one. Consequently, the cation radical of the parallel structure of the open-ring isomer is not produced.

Because the only major difference between the parallel and antiparallel structures is the different dihedral angle between the five-membered carbon ring and one of the thiophenes, the π -conjugation of the parallel and antiparallel structures are almost the same. Therefore, we can expect that the ESR spectra of these structures are similar. It is thus very likely that we found the disagreement between the calculated ESR spectrum for the parallel structure and the experimental one only because the average of the hfcc over the puckering has not been taken into account. However, unlike the antiparallel structure, the parallel structure of **1a** does not have a convenient average structure over puckering, which prevents us from confirming the similarity of the ESR spectra of these two structures by simple calculations.

The latter explanation in terms of the kinetics is given as follows. The isomerization initially takes place from the closed-ring isomer to the antiparallel structure of the open-ring isomer after the closed-ring isomer is oxidized. Then the isomerization between the parallel and antiparallel structure of the open-ring

isomer occurs by the thermal fluctuation. If the time scale of the isomerization is much slower than the decay time of the cation radical to the neutral one, the cation radical of the parallel structure of the open-ring isomer will not be produced. The free energy barriers between the antiparallel structure to the parallel structure in the neutral and cationic state are calculated by the B3LYP/cc-pVDZ in the gas phase, and those are 8.3 and 13.0 kcal/mol, respectively. Because the free energy barrier of the cationic state is larger than that of the neutral state, the time scale of the isomerization in the cationic state is expected to be much slower than that in the neutral state. The comparison of the time scale, however, requires more detailed experimental and theoretical analysis, and it is beyond the scope of this paper.

In either case, it does not affect our conclusion; the experimental ESR spectrum is due to the mixture of the open- and closed-ring isomers.

5. Conclusion

Usually, the calculations of the hfcc's are performed for small molecules or moderate sized molecules with high symmetries or with simple structures. The good agreements between the hfcc's determined experimentally and those determined by the B3LYP calculations are reported only for the molecules with small or simple structures. On the other hand, the underestimation of the exchange interaction for large distance in the conventional DFT²⁹ might have some impact on the determination of the hfcc's of large molecules. Nevertheless, we assert that the conclusion given here is solid by the fact that the difference of the width of the ESR spectra between the open- and closed-ring isomers is caused by the difference of the π -conjugation in these two isomers, which is unaffected by the drawback of the conventional DFT.

The C_2 symmetry is imposed in our calculations. The use of the symmetric structure corresponds to the zeroth-order approximation of the averaging of the hfcc over the time of the ESR measurement. Consequently, all 16 hfcc's give different values in the nonsymmetric structure, whereas we have 2 sets of 8 hfcc's in the symmetric structure, which leads to a smaller number of peaks in the ESR spectra. This is why the number of peaks is reduced in Figure 4(b) (Figure S3(b)) compared to Figure 4(a) (Figure S3(a)). To have a better approximation, we need to calculate the potential energy surface and obtain each minimum and perform the average including the vibrations around the minima by assuming the Boltzmann distribution. This is one of the reasons we still have minor discrepancies between the computational and the experimental results in Figure 6. For the simplicity of the discussion above, we do not consider the average over the rotation of the methyl group. This does not affect our conclusion, because the rotation of the methyl group does not change the spectral width as discussed in the Supporting Information.

In conclusion, we found that the ratio of the open- and closed-ring isomers of the cationic diarylethene during electrochemical oxidation reaction is 4:1. The ratio will depend on the experimental condition, such as, the concentration of the closed-ring isomer of the diarylethene, which is important for the reaction kinetics. Due to the strong dependence of the hfcc's on the structure of the molecule, we obtain the complicated ESR spectra (Figure 4(a)). The computational ESR spectrum, however, becomes simple by imposing the C_2 symmetry on the structure of the diarylethene as in Figure 4(b). This corresponds to an approximation of the averaging procedure of the hfcc's over the structures of the energy minima related to the puckering motion. We found that the spectral width of the ESR is significantly different between the open- and close-ring isomers. This is due to the difference in the π -conjugation between two isomers. The ESR spectral width analysis could, thus, be used to identify the isomerization of the radical species, which involves the change of the π -conjugation. Based on the analysis, we then reproduce the experimental spectrum as the mixture of the open- and closed-ring isomers of the diarylethenes as shown in Figure 6. The excitation energies of the cationic diarylethene are further identified by the SAC-CI calculations.

Acknowledgment. This research was supported by CREST, JST.

Supporting Information Available: Complete reference Gaussian, dependence of hfcc's on rotation of methyl groups, and dependence of ESR spectra on basis set. This material is available free of charge via the Internet at <http://pubs.acs.org>.

References and Notes

- (1) (a) Slichter, C. P. *Principles of magnetic resonance*, 3rd ed.; Springer: Berlin, 1996. (b) *Calculation of NMR and EPR Parameters: Theory and Applications*; Kaupp, M., Bühl, M., Malkin, V. G., Eds.; Wiley-VCH: Weinheim, 2004.
- (2) *Encyclopedia of Nuclear Magnetic Resonance. Advances in NMR*; Grant, D. M., Harris, R. K., Eds.; John Wiley & Sons: Chichester, 2002; Vol. 9.
- (3) (a) London, F. *J. Phys. Radium* **1937**, 8, 397. (b) Gauss, J. *J. Chem. Phys.* **1993**, 99, 3629. (c) Kutzelnigg, W. *Isr. J. Chem.* **1980**, 19, 193. (d) Malkin, V. G.; Malkina, O. L.; Casida, M. E.; Salahub, D. R. *J. Am. Chem. Soc.* **1994**, 116, 5898.
- (4) (a) Irie, M. *Chem. Rev.* **2000**, 100, 1685. (b) Irie, M.; Uchida, K. *Bull. Chem. Soc. Jpn.* **1998**, 71, 985.
- (5) (a) Koshido, T.; Kawai, T.; Yoshino, K. *J. Phys. Chem.* **1995**, 99, 6110. (b) Peters, A.; Branda, N. R. *J. Am. Chem. Soc.* **2003**, 125, 3404. (c) Peters, A.; Branda, N. R. *Chem. Commun.* **2003**, 954. (d) Zhou, X.-H.; Zhang, F.-S.; Yuan, P.; Sun, F.; Pu, S.-Z.; Zhao, F.-Q.; Tung, C.-H. *Chem. Lett.* **2004**, 33, 1006.
- (6) Moriyama, Y.; Matsuda, K.; Tanifuji, N.; Irie, S.; Irie, M. *Org. Lett.* **2005**, 7, 3315.
- (7) Becke, A. D. *J. Chem. Phys.* **1993**, 98, 5648.
- (8) Eriksson, L. A. ESR Hyperfine Calculations. In *Encyclopedia of Computational Chemistry*; Schleyer, P. R., Ed.; Chichester: Wiley: 1998; Vol. 2, p 952.
- (9) (a) Zuilhof, H.; Dinnocenzo, J. P.; Reddy, A. C.; Shaik, S. *J. Phys. Chem.* **1996**, 100, 15774. (b) Nguyen, M. T.; Creve, S.; Vanquickenborne, L. G. *J. Phys. Chem. A* **1997**, 101, 3174. (c) Jaszewski, A. R.; Siatecki, Z.; Jezierska, J. *Chem. Phys. Lett.* **2000**, 331, 403. (d) Liu, Y.-J.; Huang, M.-B. *J. Mol. Struct. (THEOCHEM)* **2001**, 536, 133. (e) Kalina, O. G.; Tumanskii, B. L.; Chistyakov, A. L.; Stankevich, I. V.; Birkett, P. R.; Taylor, R. *Chem. Phys. Lett.* **2003**, 380, 491. (f) Leopoldini, M.; Marino, T.; Russo, N.; Toscano, M. *Theor. Chem. Acc.* **2004**, 111, 210.
- (10) Rakitin, A. R.; Yff, D.; Trapp, C. *J. Phys. Chem. A* **2003**, 107, 6281.
- (11) Sekino, H.; Bartlett, R. J. *J. Chem. Phys.* **1985**, 82, 4225.
- (12) Becke, A. D. *Phys. Rev. A* **1988**, 38, 3098.
- (13) Lee, C.; Yang, W.; Parr, R. G. *Phys. Rev. B* **1988**, 37, 785.
- (14) Frisch, M. J.; et al. *Gaussian 03, Revision C.02*; Gaussian, Inc.: Wallingford, CT, 2004.
- (15) (a) Dunning, T. H., Jr. *J. Chem. Phys.* **1989**, 90, 1007. (b) Kendall, R. A.; Dunning, T. H., Jr.; Harrison, R. J. *J. Chem. Phys.* **1992**, 96, 6796. (c) Woon, D. E.; Dunning, T. H., Jr. *J. Chem. Phys.* **1993**, 98, 1358.
- (16) (a) Krishnan, R.; Binkley, J. S.; Seeger, R.; Pople, J. A. *J. Chem. Phys.* **1980**, 72, 650. (b) Frisch, M. J.; Pople, J. A.; Binkley, J. S. *J. Chem. Phys.* **1984**, 80, 3265.
- (17) (a) Chang, S. Y.; Davidson, E. R.; Vincow, G. *J. Chem. Phys.* **1970**, 52, 5596. (b) Chipman, D. M. *J. Chem. Phys.* **1983**, 78, 3112. (c) Ellinger, Y.; Puzat, F.; Barone, V.; Douady, J.; Subra, R. *J. Chem. Phys.* **1980**, 72, 6390. (d) Barone, V.; Grand, A.; Minichino, C.; Subra, R. *J. Chem. Phys.* **1993**, 99, 6787. (e) Barone, V.; Adamo, C.; Grand, A.; Subra, R. *Chem. Phys. Lett.* **1995**, 242, 351. (f) Barone, V.; Adamo, C.; Grand, A.; Subra, R. *Chem. Phys. Lett.* **1995**, 246, 53.
- (18) (a) Nakatsuji, H. *Chem. Phys. Lett.* **1978**, 59, 362. (b) Nakatsuji, H.; Hirao, K. *J. Chem. Phys.* **1978**, 68, 2053. (c) Nakatsuji, H. *J. Chem. Phys.* **1991**, 94, 6716.
- (19) (a) Stratmann, R. E.; Scuseria, G. E.; Frisch, M. J. *J. Chem. Phys.* **1998**, 109, 8218. (b) Bauernschmitt, R.; Ahlrichs, R. *Chem. Phys. Lett.* **1996**, 256, 454. (c) Casida, M. E.; Jamorski, C.; Casida, K. C.; Salahub, D. R. *J. Chem. Phys.* **1998**, 108, 4439.
- (20) Goldberg, A.; Murakami, A.; Kanda, K.; Kobayashi, T.; Nakamura, S.; Uchida, K.; Sekiya, H.; Fukaminato, T.; Kawai, T.; Kobatake, S.; Irie, M. *J. Phys. Chem. A* **2003**, 107, 4982.
- (21) Equation 3 is for a system which has atoms with a nuclear spin of 0 or 1/2.
- (22) (a) McConnell, H. M. *J. Chem. Phys.* **1956**, 24, 764. (b) McConnell, H. M.; Chesnut, D. B. *J. Chem. Phys.* **1958**, 28, 107.
- (23) Fukaminato, T.; Kawai, T.; Kobatake, S.; Irie, M. *J. Phys. Chem. B* **2003**, 107, 8372.
- (24) Hirata, S.; Lee, T. J.; Head-Gordon, M. *J. Chem. Phys.* **1999**, 111, 8904.
- (25) Rinkevicius, Z.; Tunell, I.; Salek, P.; Vahtras, O.; Ågren, H. *J. Chem. Phys.* **2003**, 119, 34.
- (26) Kaieda, T.; Kobatake, S.; Miyasaka, H.; Murakami, M.; Iwai, N.; Nagata, Y.; Itaya, A.; Irie, M. *J. Am. Chem. Soc.* **2002**, 124, 2015.
- (27) Uchida, K.; Guillaumont, D.; Tsuchida, E.; Mochizuki, G.; Irie, M.; Murakami, A.; Nakamura, S. *J. Mol. Struct. (THEOCHEM)* **2002**, 579, 115.
- (28) Asano, Y.; Murakami, A.; Kobayashi, T.; Kobatake, S.; Irie, M.; Yabushita, S.; Nakamura, S. *J. Mol. Struct. (THEOCHEM)* **2003**, 625, 227.
- (29) (a) Almladh, C.-O.; Pedroza, A. C. *Phys. Rev. A* **1984**, 29, 2322. (b) Levy, M.; Perdew, J. P.; Sahni, V. *Phys. Rev. A* **1984**, 30, 2745. (c) Iikura, H.; Tsuneda, T.; Yanai, T.; Hirao, K. *J. Chem. Phys.* **2001**, 115, 3540.